Research Square

Preprints are preliminary reports that have not undergone peer review.
They should not be considered conclusive, used to inform clinical practice,
or referenced by the media as validated information.

An interactive virtual reality-based tutorial system for the heat equation and visualization of temperature distribution graphs

Kalpana Shankhwar

kalpana@iiitd.ac.in

Indraprastha Institute of Information Technology Delhi https://orcid.org/0000-0002-6171-8927

Research Article

Keywords: Virtual reality, heat equation, Fourier series approximation, 3D graph visualization, 3D mesh generation, bare-hand interaction.

Posted Date: July 13th, 2026

DOI: https://doi.org/10.21203/rs.3.rs-10312400/v1

License: This work is licensed under a Creative Commons Attribution 4.0 International License.
Read Full License

Additional Declarations: The authors declare no competing interests.

An interactive virtual reality-based tutorial system for the heat equation and visualization of temperature distribution graphs

Abstract: Visualizing technical concepts in engineering education is a common challenge that students face, often limiting students' ability to apply classroom knowledge to solve real-world problems. Virtual reality (VR) has emerged as an innovative tool that offers an immersive and interactive learning environment that can enhance the comprehension of complex topics that require 3D visualization. The aim of this study is to develop a VR-based tutorial system designed to help students understand the complex heat equation and visualize its solution in 3D. The VR-based tutorial system introduces an intuitive, immersive user interface that enables users to learn the fundamentals of the heat equation and visualize temperature distribution graphs generated by Fourier series approximations. The user can attend the heat equation tutorial with step-by-step guidance through the visual cues and instructional prompts. A user study was conducted to examine the impact of the VR-based learning environment on students' comprehension and knowledge retention. The user study results indicate that participants using the VR tutorial performed significantly better in terms of knowledge retention than those who learned the heat equation through a conventional classroom method. In addition to this, the usability of the developed system was validated using the system usability scale (SUS) analysis.

Keywords: Virtual reality, heat equation, Fourier series approximation, 3D graph visualization, 3D mesh generation, bare-hand interaction.

1. Introduction

Technical and engineering education involving complex mathematics often struggles with effectively conveying concepts, particularly when the visualization of multidimensional transformations is required (Oje et al. 2023; Streveler et al. 2008). In engineering education, the heat equation is one such topic that also faces this challenge. The heat equation, which is a parabolic partial differential equation (PDE), explains how the temperature changes within a specific area as time progresses (Gorguis Chan 2008). Conventional teaching methodologies rely heavily on symbolic, static 2D representations of the heat equation, without the physical intuition and visualization as underlying requirements.

One of the most prevailing challenges is that the students lack a deep understanding of deriving and solving the heat equation and retaining the knowledge. The heat equation is generally solved using the Fourier series approximation, which yields the temperature distribution graphs. However, in real-world scenarios, the temperature distribution is inherently a 3D phenomenon, with spatial dimensions alongside temporal variations. Due to the non-availability of the dynamic visualization tools, students' understanding of the transition from mathematical derivations to real-world 3D heat flow remain limited (Eynde et al. 2020; Strzys et al. 2018).

Engineering education has traditionally relied on static diagrams and images, often accompanied by laboratory experiments for practical exposure and hands-on learning. However, these methods are both time-consuming and resource-intensive. For instance, in physics, conventional pedagogy often struggles to effectively convey the 3D structures of crystals, making it difficult for students to visualize and understand abstract concepts (Alipour et al. 2024). Engineering education involves numerous complex topics that are difficult to teach effectively using traditional classroom methods. As a result, laboratory experiments become essential for effective learning and knowledge retention; however, they can be costly and potentially hazardous (Guzmán et al. 2024). Likewise, in mathematics, static textbook-based teaching often diminishes motivation to learn and may be insufficient in developing spatial reasoning, preventing learners from internalizing abstract geometric ideas (Su et al. 2022). Apart from this, in building-service engineering, traditional lecture-based instruction lacks the interactivity needed to help students meaningfully understand complex models like Fanger's thermal comfort theory (Hou 2023).

In engineering courses such as heat transfer, thermodynamics, and mathematics, the solution of the heat equation, which describes how temperature changes over time and space, is traditionally

taught through derivations and static 2D figures. This approach restricts the students from understanding how 1D Fourier-based solutions correspond to complex real-world heat transfer phenomena. Visualization-assisted teaching methods have shown improved problem-solving performance; however, restricted simulation capabilities and the lack of interactive 3D learning environments constrain students' ability to achieve a conceptual depth and practical understanding (Eynde et al. 2020).

Extended reality (XR), which encompasses virtual reality (VR), augmented reality (AR), and mixed reality (MR), is an innovative tool capable of providing experiential learning through hands-on experiences in an immersive, interactive, and engaging environment. It can allow students to explore how a 1D heat equation transforms into a Fourier series and then into 2D and 3D temperature distribution graphs with a stereoscopic view. For example, Shankhwar Smith (2022) developed an MR-based welding training and tutorial system to teach the fundamentals of welding technology, which proved to be a substantial tool in significantly improving the knowledge retention among students due to the experiential learning platform. Therefore, by leveraging VR technology, the fundamental knowledge of the heat equation can be presented in a stereoscopic environment in an intuitive way. Thus, this study aims to develop an educational system using VR technology to teach the heat equation, enabling students to comprehend the phenomena of heat propagation over time in an immersive environment. This paper is organized as follows. Section 2 provides related work. Section 3 presents the system architecture. Section 4 describes the design and implementation of the VR system for the heat equation tutorial. Section 5 discusses the user study. Section 6 presents the user study results and their analysis. Section 7 provides the discussion. Lastly, Section 8 offers conclusions and future work.

2. Related work

XR technology has enabled students to gain a deeper understanding of complex topics by visualizing them in immersive environments. It is widely recognized that students learn new concepts in any discipline more effectively when they can apply them through practical activities. Such hands-on engagement can be perceived as a form of experiential learning (Macariu et al. 2020; Shankhwar et al. 2022). Previous studies have proven the effectiveness of XR technology in grasping fundamental knowledge on various topics (Ghazali et al. 2024; Han 2022; Turkan et al. 2017).

XR has been employed to develop training and tutorial systems for K-12 and engineering education. For example, Simonetti et al. (2020) developed a VR-based system to teach analytical-geometric structures in mathematics, demonstrating that immersive environments can significantly improve students' understanding of the concepts. Cheong et al. (2023) used a Google Cardboard to display 3D graphs from functions of two variables and assessed its usability for the visualization of multivariable calculus. Ghazali et al. (2024) implemented an in-house VR laboratory for first-year students of electronics engineering to provide better visualization and interaction on the subject matter of electromagnetism. The research findings revealed a positive attitude of students towards learning through hands-on experience in the VR laboratory. Matovu et al. (2024) investigated the influence of complex chemistry learning activities in immersive VR on the students' perception. The study found improved engagement and extensive student interaction through the exploration of 3D representations from multiple angles. Castillo et al. (2025) presented a framework to teach the concept of projectile motion using VR. The user study results indicated the system's efficiency in helping students understand the context.

Apart from VR, some studies have displayed the potential of AR in education. For instance, Turkan et al. (2017) developed an AR-based tutorial system to study structural analysis that is taught in every civil engineering program. The study indicated that 3D visualization and interactive features could support students' constructive engagement and information retention. Macariu et al. (2020) employed AR in chemistry education. The user study results showed that the system could respond to students' curiosity and helped them develop logical thinking in an interactive way without any extra effort of memorizing the concepts. Singh et al. (2024) developed an AR-based application called 'Hyperspace' to teach trigonometry. The procedural content generation algorithm and computer graphics are used to dynamically generate trigonometric functions in AR, thereby significantly enhancing students' spatial skills and conceptual knowledge in trigonometry. Geng et al. (2026) validated the impact of adopting AR smart glasses on young children's engagement in science learning. The students displayed enhanced social engagement, fostered collaboration, and engaged in peer communication through shared visual experiences.

In addition to AR, some prior studies have demonstrated the benefits of using MR in education. For example, Lindgren et al. (2016) investigated how students' full-body movements could be used to interact with and learn about scientific concepts within an MR environment. The findings demonstrated that this form of embodied interaction within the MR simulation resulted in higher

levels of student engagement. Frank Kapila (2017) presented a tangible application of MR in engineering education, deployed on a mobile device, which overlays interactive virtual graphics onto the physical laboratory experiment. The students could directly manipulate the virtual elements on the screen, which, in turn, altered the behavior of the real-world test bed in real time. The system helped students understand the complex concepts in dynamic systems and control. Shankhwar Smith (2022) presented an MR-based welding tutorial system that supports experiential learning of fundamental welding concepts with realistic hands-on practice, resulting in better knowledge retention than traditional classroom instruction.

Prior studies have consistently reported significant pedagogical benefits of using XR technologies in education. The 3D representation of complex topics in immersive and risk-free environments and hands-on exercises tremendously improves learning and knowledge retention among students. In addition, students' competitiveness with their peers is increased. Although XR has been employed across a wide range of engineering education domains, to the best of our knowledge, no literature was found to demonstrate an intuitive interaction with 3D graphs in real time by controlling variables of mathematical expressions. In addition to the 3D graph manipulation, previous studies lack the application of a custom shader to display the heat map on the surface of a 3D geometry in XR-based education systems. Furthermore, most XR-based education systems rely on mobile devices for deployment, while only a few utilize head-mounted displays and lack a natural, gesture-based bare-hand interaction with the system.

Among XR technologies, VR immerses users in a fully virtual environment, providing deep engagement and spatial presence that are crucial for understanding complex and abstract concepts, especially in STEM fields. The fully immersive nature of VR minimizes external distractions, allowing students to concentrate deeply on the study material, creating stronger feelings of presence and engagement than AR (Huang et al. 2019). Moreover, VR's controlled environment enables learners to develop practical skills safely, which is less feasible with AR or MR setups. Therefore, VR has been preferred in the proposed system, which emphasizes practical usability through a learning-by-doing approach. The proposed system employs VR to develop a tutorial that teaches the fundamentals of the heat equation and its solution using the Fourier series approximation. The temperature distribution graphs obtained from the Fourier series approximation are dynamically generated using computer graphics.

3. System Architecture

The flow chart of the VR tutorial system is shown in Fig. 1. The heat equation tutorial system is implemented in a VR environment. The purpose of VR system is to demonstrate the fundamentals of the heat equation. The tutorial begins in a VR classroom that resembles a traditional classroom, with a board showcasing the basic mathematical expressions for the 1D heat equation, Fourier series, and corresponding waveform types.

After reading the content on the board, an interactive user interface (UI) presenting a detailed explanation of the heat equation appears on the user's desk. The reading content consists of the objective, initial conditions, boundary conditions, and the general heat equation for a metal bar. Following this introductory stage, the system guides the user through three different waveforms, including square, sawtooth, and triangular waveforms, used to approximate the solution to the heat equation using the Fourier series expansion.

The user then selects a waveform from the list and navigates to a UI with a slider that allows them to adjust the number of terms n in the Fourier series expansion. Consequently, the system generates and displays a 2D graph representing temperature as a function of the metal bar length, along with a 3D graph illustrating the temperature distribution across the bar with respect to both length and time. Finally, the user can dynamically select the waveform type and number of terms to observe the resulting changes in both graphs. This interactive feature enables the user to explore the effect of series truncation on the accuracy and behavior of the solution.

The system architecture of the VR system of the heat equation is depicted in Fig. 2. The VR system is deployed on a Meta Quest 3 VR head-mounted display (HMD) to display the heat equation tutorial. An in-built vision-based tracking method in Meta Quest is used to detect and track the user's hand gestures. The user interacts with the UI elements using natural hand gestures. The interactions involve pressing a button to trigger an event or dragging a virtual slider to adjust a parameter.

The system is built on a high-performance computer equipped with an AMD Ryzen 9 7950X 16-core processor running at 4.50 GHz, 32 GB of DDR5 RAM (5200 MT/s), and a dedicated Nvidia RTX 4060Ti GPU with 16 GB of VRAM. The Meta All-in-One SDK version v71 is used for VR development. The scripts are written in C# using Unity 2022.3.60f1.

The VR system is divided into four modules: information module, interaction module, computational module, and rendering module. The information module provides the fundamentals

of the heat equation and the Fourier series approximation, along with step-by-step guidance to help users explore the tutorial. The interaction module allows users to interact with the system using the UI elements to intuitively visualize the effects of their input commands. The computational module computes the Fourier series approximation of the heat equation based on the selected waveform and number of terms. The rendering module converts the mathematical models computed by the computational module into 3D representations, allowing users to observe the evolution of temperature over length and time.

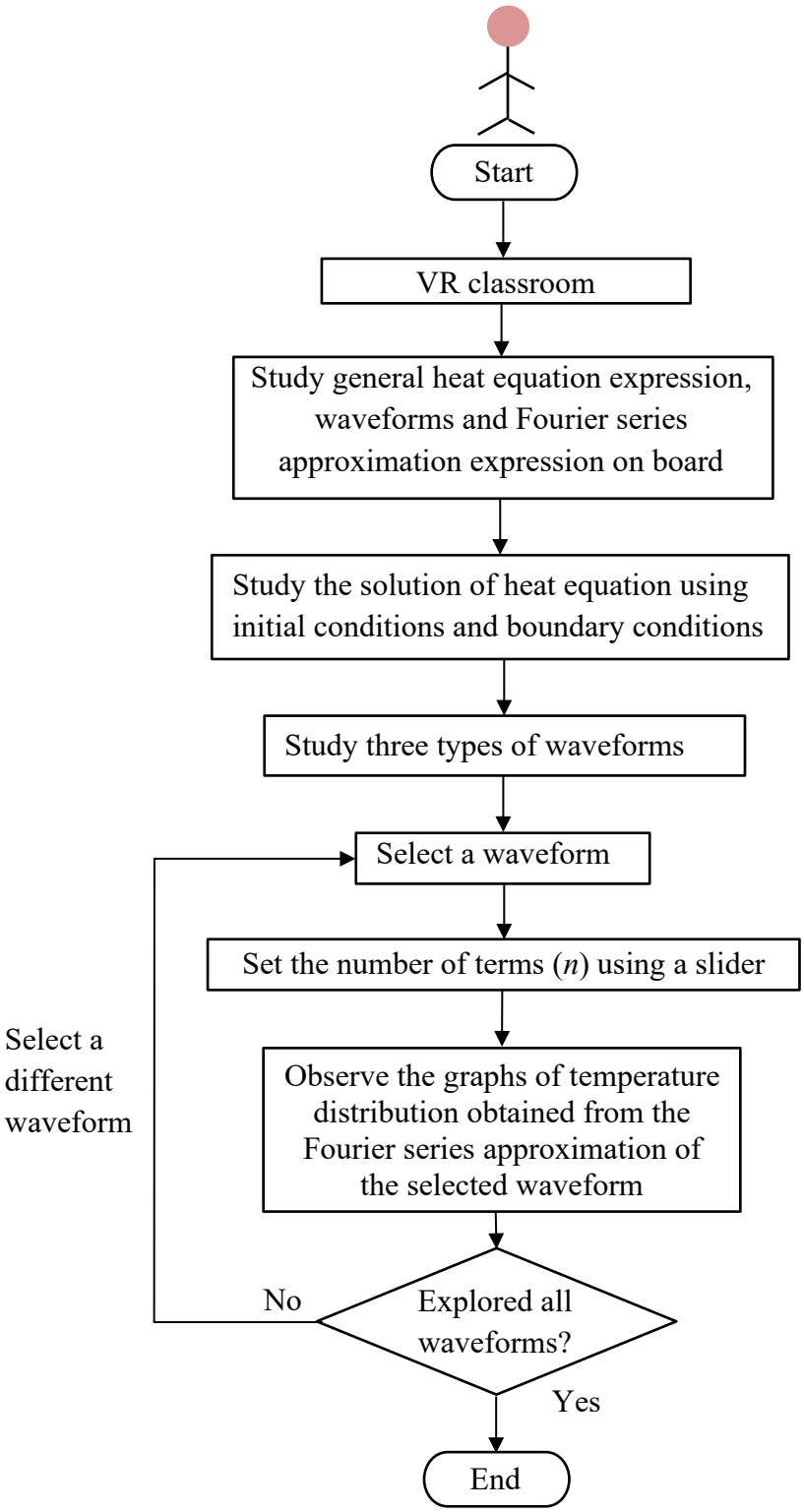


Fig. 1. Flowchart of the heat equation tutorial in VR.

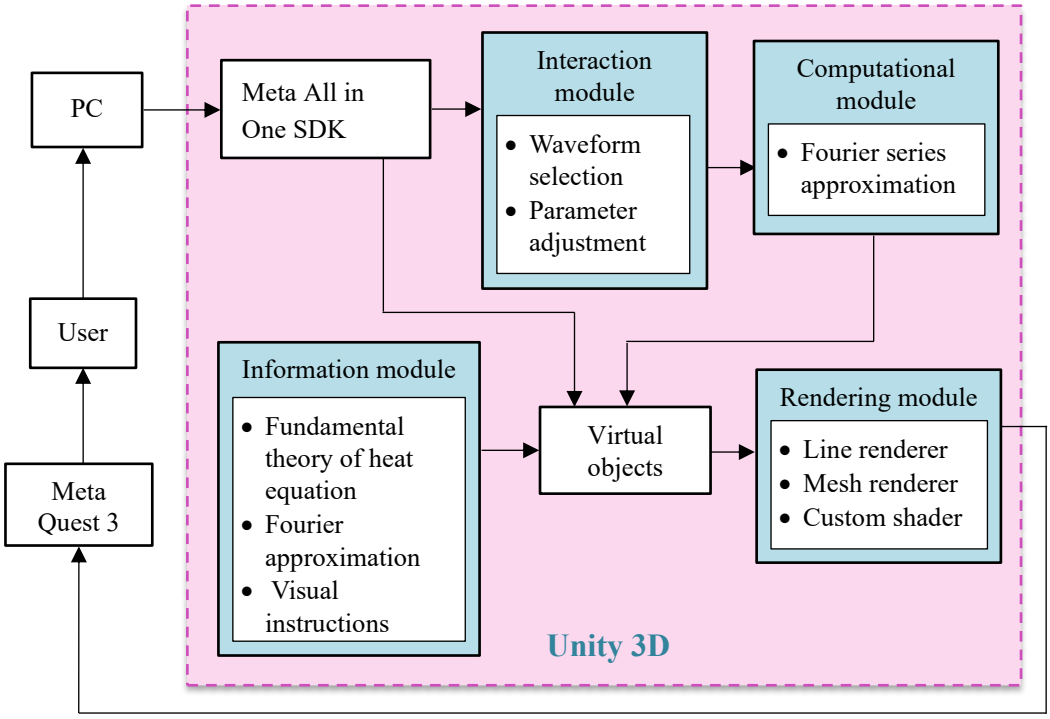


Fig. 2. System Architecture.

4. System implementation

4.1 Heat equation

This work focuses on developing a heat equation tutorial system using VR technology to understand 1D heat conduction in a metal bar. Heat transfer is accompanied by space-time variation of temperature, and the analytical computations for the amount of heat exchange in three dimensions lie in determining a mathematical relation for the temperature field. Under unsteady thermal conditions, the temperature of the system changes continuously with time, which is a function of space and time (Kumar 2008).

$$u = f(x, y, z, t); \frac{du}{dt} \neq 0 \tag{1}$$

The general heat conduction equation for self-generating, unsteady-state three-dimensional heat flow through an isotropic material is represented by Eq. 2.

$$\frac{\partial^2 u}{\partial x^2} + \frac{\partial^2 u}{\partial y^2} + \frac{\partial^2 u}{\partial z^2} + \frac{q_g}{k} = \frac{1}{\alpha}\frac{\partial u}{\partial t} \tag{2}$$

Where u is temperature, q_g is heat generated per unit volume and per unit time, k is thermal conductivity, and α is thermal diffusivity. Under steady thermal conditions, the temperature at each point in the system remains constant over time, and it is a function of only the space co-ordinates as shown below.

$$u = f(x, y, z);\ \frac{du}{dt} = 0 \tag{3}$$

For 1D heat flow under steady thermal conditions with no internal heat generation, Eq. 2 takes the form as represented below.

$$\frac{\partial u}{\partial t} = \alpha \frac{\partial^2 u}{\partial x^2} \tag{4}$$

The heat equation is a second-order partial differential equation. To solve the heat equation, the Fourier series is used with initial and boundary conditions. The initial condition is specified by $f(x)$, which represents the initial temperature profile along the bar.

$$u(x, 0) = f(x) \text{ for } 0 \leq x \leq L \tag{5}$$

Where L represents the length of the bar. The boundary condition indicates that the temperature at both ends of the bar is zero for all times $t > 0$.

$$u(0, t) = 0 \text{ and } u(L, t) = 0 \tag{6}$$

To analyze the effects of initial conditions, three types of initial temperature distributions are employed. First, the square wave, in which the temperature alternates discretely between two values along the bar (Fig. 3(a)). This results from the heat supply at both ends of the bar. Second, the sawtooth wave, where temperature increases linearly and resets, producing a gradual and progressive dissipation of heat (Fig. 3(b)). This results from the heat application at one end of the bar. Third, the triangular wave, with the temperature increasing linearly away from one end and reaching a maximum at the center, and then decreasing till the other end of the bar, resulting from the heat supply at the center. The square, sawtooth, and triangular wave functions are represented by Eqs. 7, 8 and 9, respectively.

$$f(x) = \begin{cases} 1 & for \quad 0 \leq x < 1 \\ 0 & for \quad x = 0,1 \end{cases} \tag{7}$$

$$f(x) = 1 - x \quad for\ x \in [0,1] \tag{8}$$

$$f(x) = \begin{cases} 2x & for \quad 0 \leq x < 0.5 \\ 2(1-x) & for \quad 0.5 < x \leq 1 \end{cases} \tag{9}$$

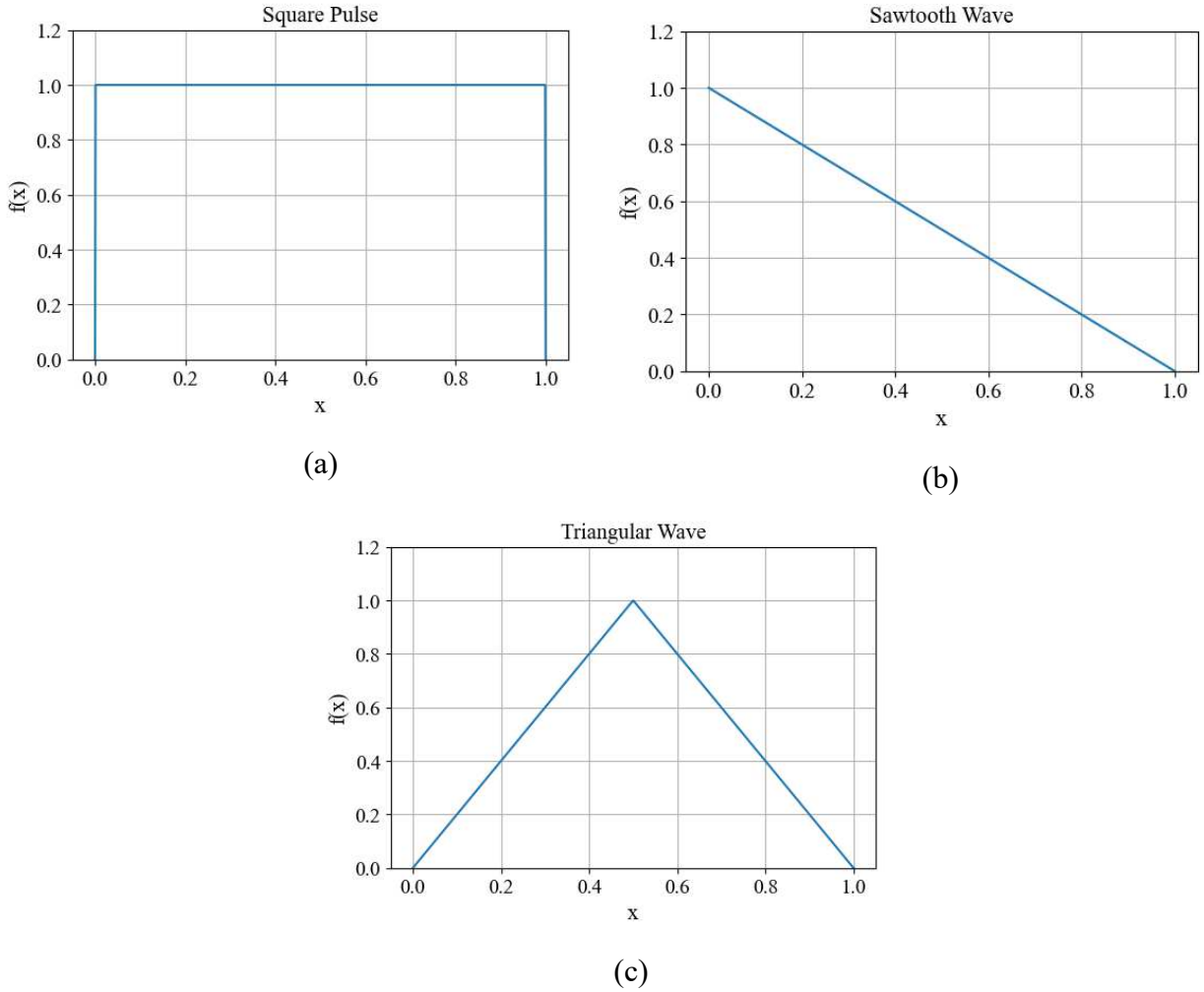


Fig. 3. Three types of waves. (a) square, (b) sawtooth, and (c) triangular wave.

The temperature distribution over the bar for three different conditions with steady state heat flow is obtained by solving Eq. 4 using a Fourier series expansion, which is shown by Eq. 10.

To further demonstrate the principle of Fourier series convergence, Fig. 4 presents the reconstructed wave functions for square, sawtooth, and triangular distributions using different numbers of terms, n = 1, 3, 10, and 100.

$$f(x) = \frac{a_0}{2} + \sum_{n=1}^{\infty} \left[a_n \cos\left(\frac{n\pi x}{L}\right) + b_n \sin\left(\frac{n\pi x}{L}\right) \right] \tag{10}$$

Upon the application of boundary conditions, the Fourier series expansion excludes the cosine term and takes the form:

$$f(x) = \frac{2}{\pi}\sum_{n=1}^{\infty}\left[b_n \sin\left(\frac{n\pi x}{L}\right)\right] \tag{11}$$

After applying square, sawtooth and triangular wave conditions, the Fourier series approximation of the heat equation is represented by Eqs. 12, 13, and 14, respectively.

$$f(x) = \frac{4}{\pi}\left(\sin(\pi x) + \frac{1}{3}\sin(3\pi x) + \frac{1}{5}\sin(5\pi x) + \ldots\right) \tag{12}$$

$$f(x) = \frac{2}{\pi}\sum_{n=1}^{\infty}\frac{1}{n}\sin(n\pi x) \tag{13}$$

$$f(x) = \frac{8}{\pi^2}\left(\sin(\pi x) + \frac{1}{3^2}\sin(3\pi x) + \frac{1}{5^2}\sin(5\pi x) + \ldots\right) \tag{14}$$

The temperature distribution along the length of the bar with steady state thermal condition is obtained by the Fourier series approximation of the heat equation and represented in Fig. 4. The principle of Fourier series convergence is demonstrated through the reconstructed waves of three types using different number of terms. The solution of the heat equation for square, sawtooth and triangular waves under transient temperature conditions is represented by Eqs. 15, 16 and 17, respectively. It indicates that each Fourier mode decays independently with time.

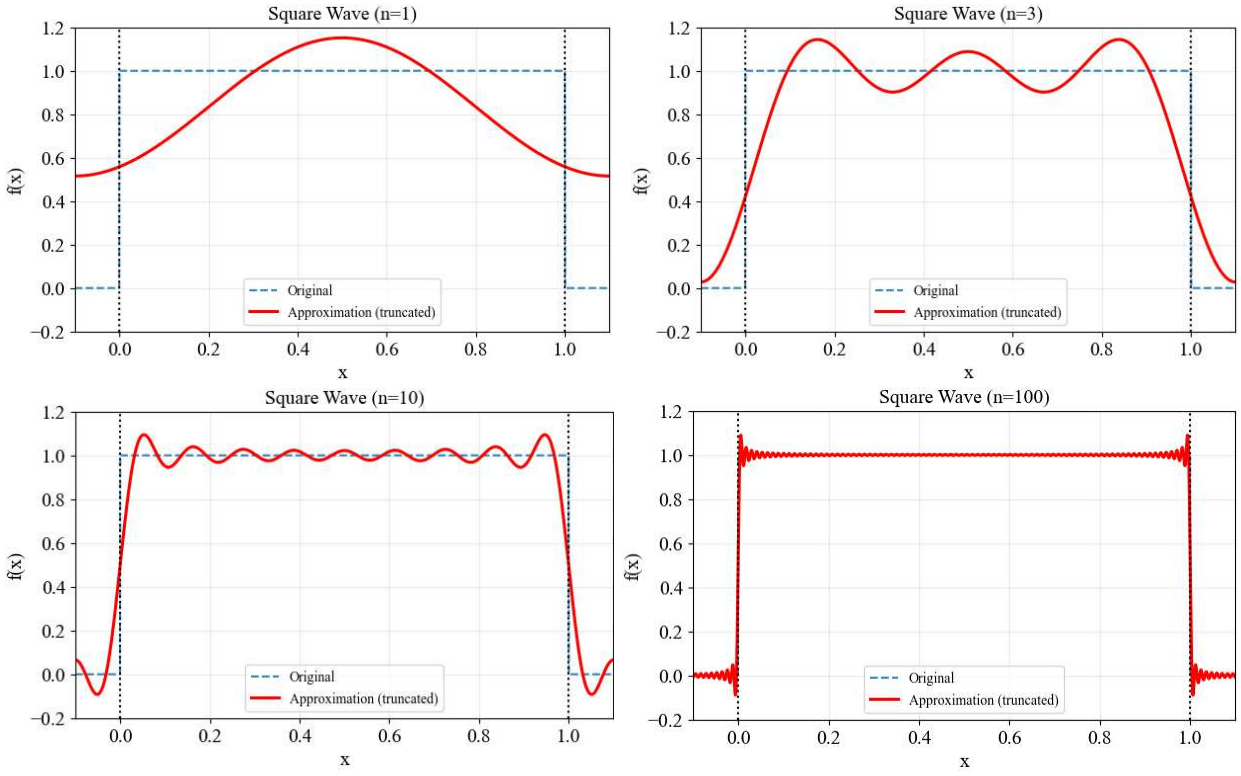
$$u(x,t) = \frac{4}{\pi}\sum_{n=1}^{\infty}\frac{1}{n}\sin(n\pi x)\exp(-\alpha(n\pi)^2\, t) \tag{15}$$

$$u(x,t) = \frac{2}{\pi}\sum_{n=1}^{\infty}\frac{1}{n}\sin(n\pi x)\exp(-\alpha(n\pi)^2 t) \tag{16}$$

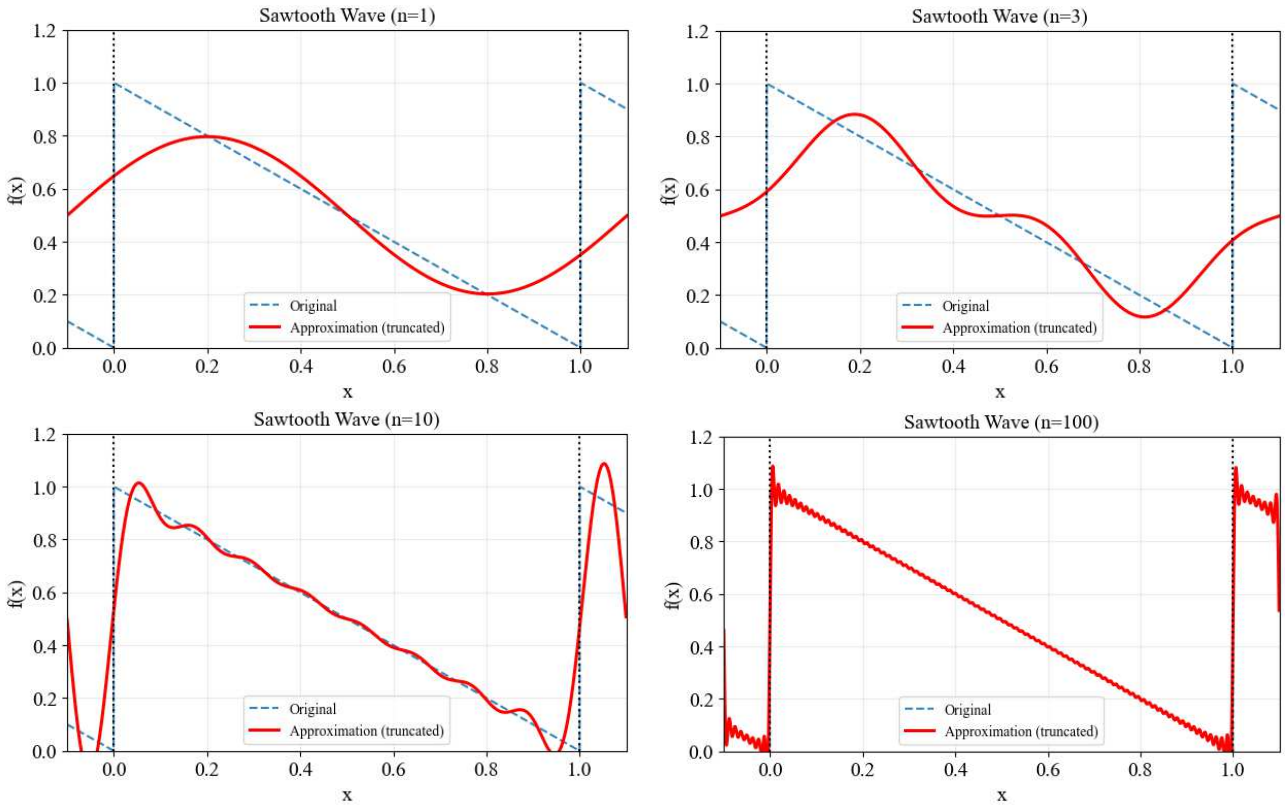
$$u(x,t) = \frac{8}{\pi^2}\sum_{n=1}^{\infty}\frac{1}{n^2}\sin(n\pi x)\exp\left(-\alpha(n\pi)^2 t\right) \tag{17}$$

It is clear from the graphs presented in Fig. 4 that the quality of approximation improves with a larger number of terms. For a low number of terms, the reconstructed curves are smooth but deviate substantially from the target function. As the number of terms increases, the approximations exhibit sharper features and progressively align more closely with the original waveforms, clearly demonstrating Fourier series convergence.

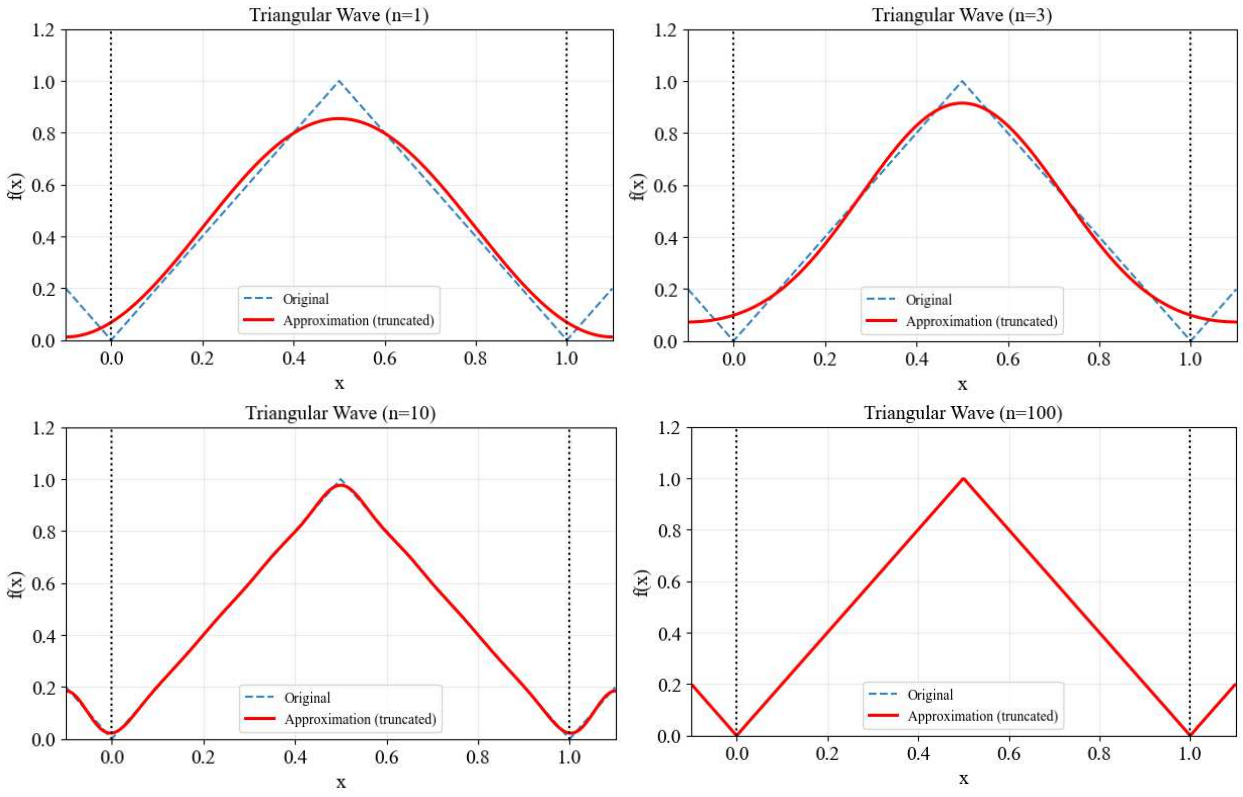
This pattern illustrates the pedagogical motivation for enabling users to interactively adjust the number of terms in the VR environment, thereby directly observing how Fourier series representations approach the analytical solution. Under unsteady state thermal conditions, the temperature distribution over the length is represented by Fig. 5. The temperature results are obtained by solving Eq. (15) – (17) using a Fourier series approximation. The x and y axes represent the bar length and temperature, respectively, as in the steady-state condition, while the z axis represents time.



(a)


Sawtooth Wave (n=1)
Sawtooth Wave (n=3)
Sawtooth Wave (n=10)
Sawtooth Wave (n=100)
Original
Approximation (truncated)
f(x)
x
0.0
0.2
0.4
0.6
0.8
1.0
1.2

(b)



(c)

Fig. 4. Temperature distribution along the bar for steady state thermal condition using Fourier series approximation of (a) square, (b) sawtooth, and (c) triangular wave for n = 1, 5, 10, 100.

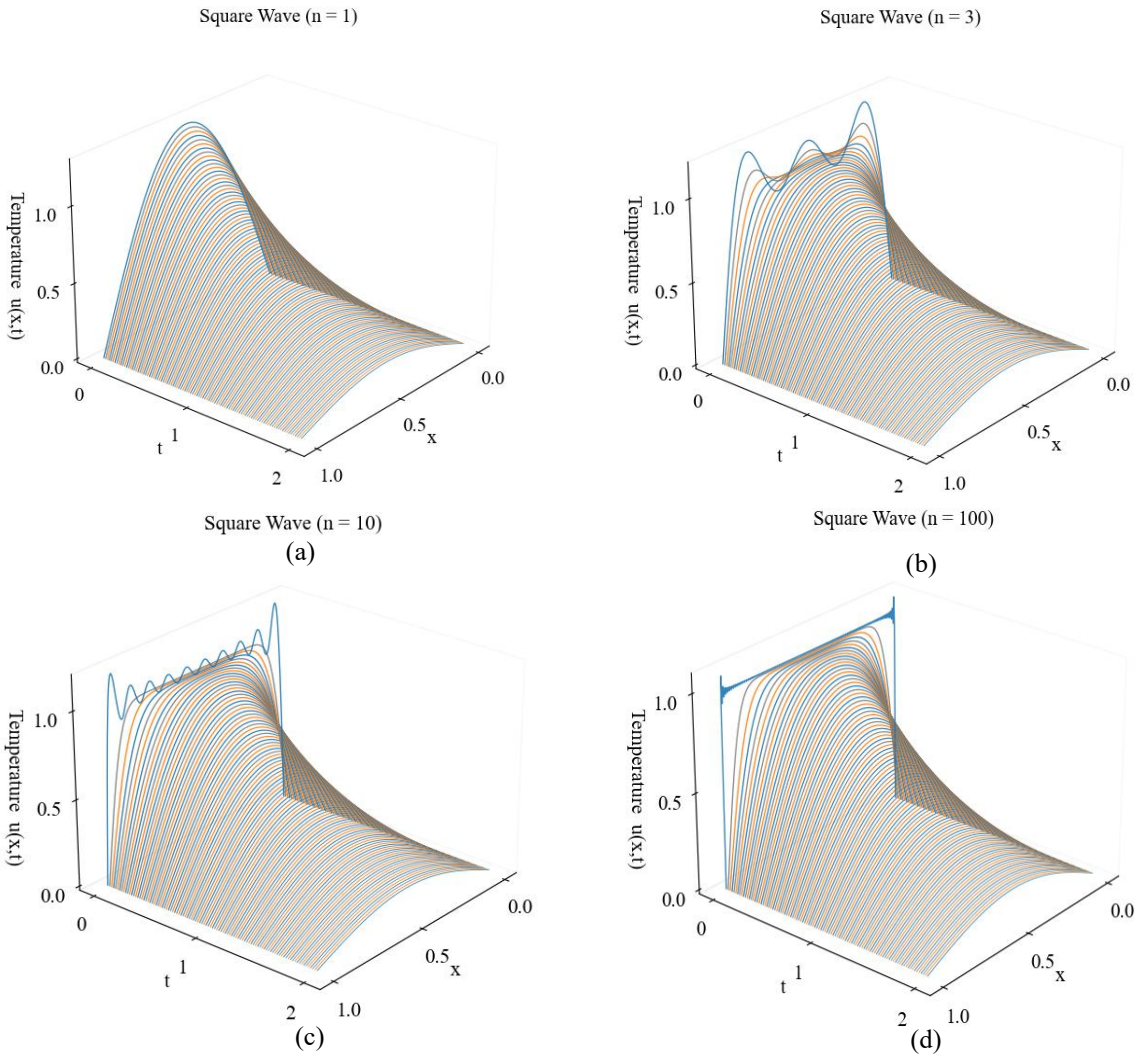
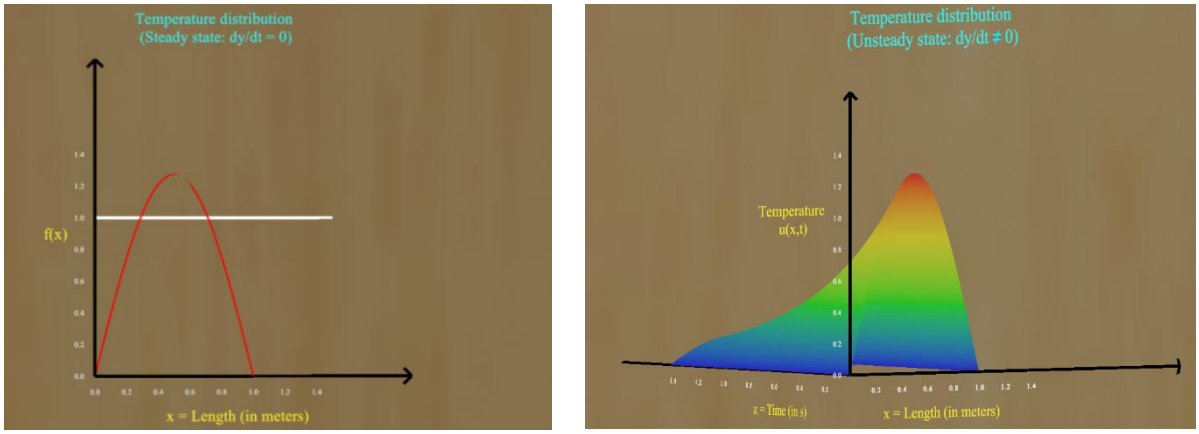


Fig. 5. Temperature distribution along the bar for unsteady state thermal condition using Fourier series approximations of square wave for (a) $n = 1$, (b) $n = 3$, (c) $n = 10$ and (d) $n = 100$.

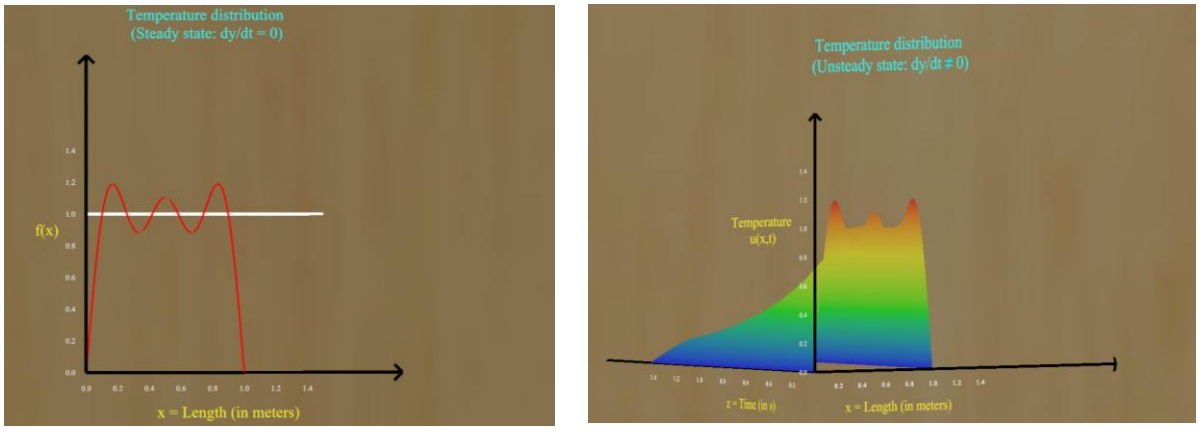
4.2 Implementation of temperature distribution graphs in VR

The VR environment for the tutorial was developed in Unity using C# for scripting. The most crucial part of the tutorial was the representation of 2D and 3D graphs of temperature distribution, with real-time manipulation of the number of terms in the Fourier series approximation. The representation of temperature distribution graphs in VR is shown in Fig. 6. The magnitude of temperature is represented via heat map with red color referring to hot (maximum temperature) and blue color referring to cold (minimum temperature). When fewer terms are used, the approximation is coarse and may exhibit visible artifacts, such as overshoots and oscillations near

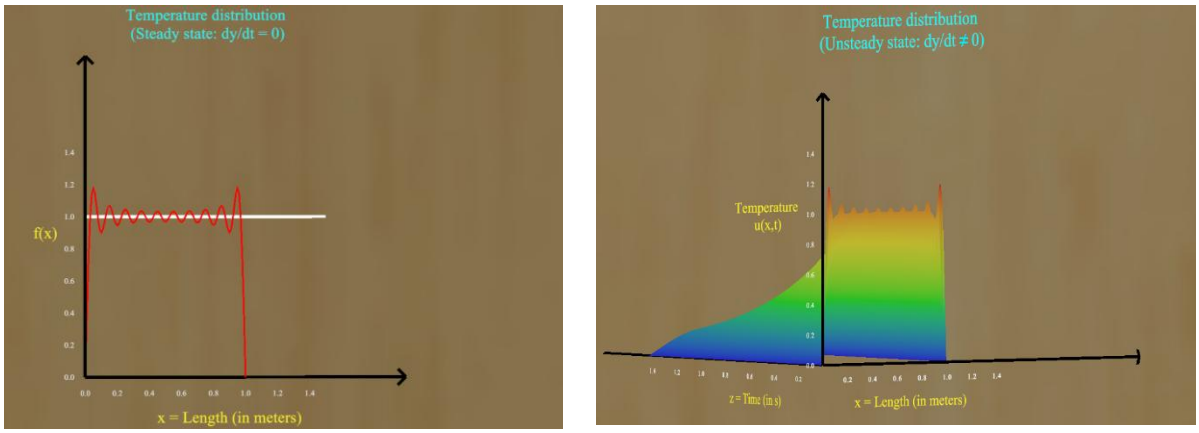
discontinuities (Cheong Koh 2018). In Fig. 6, the graphs show that a higher number of terms provides a more accurate approximation of the waveforms. To avoid jitters and rendering lag caused by computational limitations, the range of terms was set from 1 to 10. This range allows users to directly perceive how the incremental addition of terms improves the degree of approximation without incurring the cost of high-latency rendering.



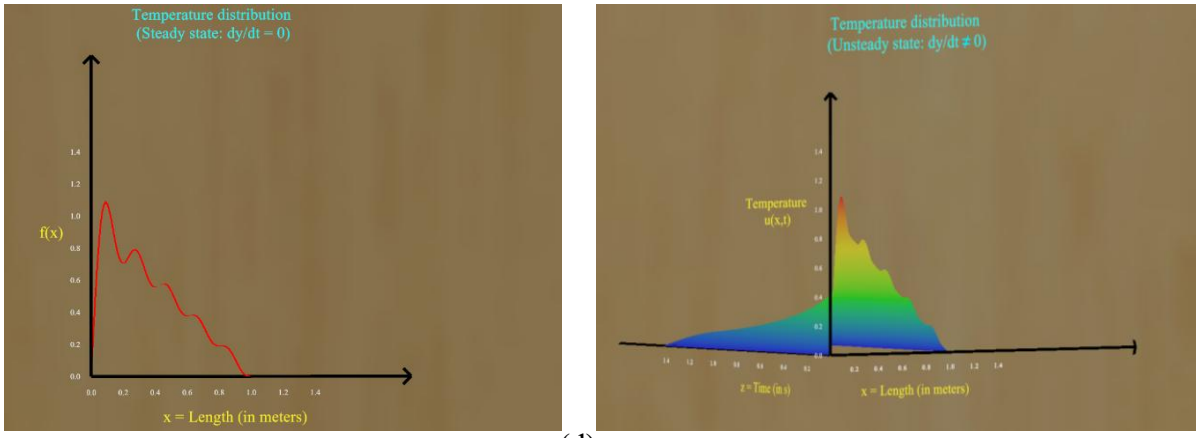
(a)



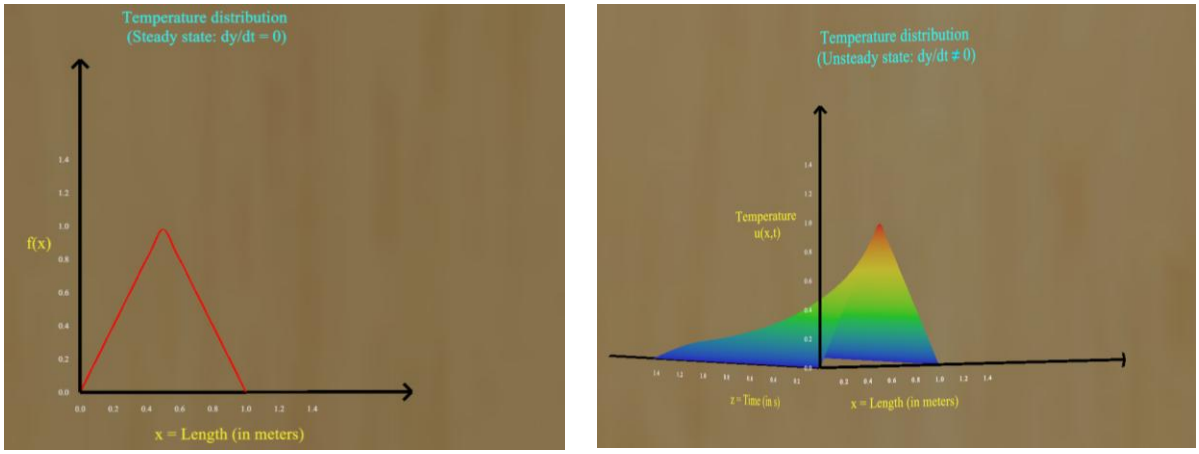
(b)



(c)



(d)



(e)

Fig. 6. Temperature distribution graphs in VR environment using Fourier approximation under steady state thermal condition represented by 2D graph and unsteady state thermal condition represented by 3D graph with (a) $n = 1$ (b) $n = 3$, (c) $n = 10$ for square, (d) $n = 10$ for sawtooth and (e) $n = 10$ for triangular wave.

Temperature distribution graphs are rendered in the VR environment using computer graphics techniques. Two primary scripts, functionally interrelated for each waveform, are written in C#, and a custom shader is developed. One script handles the computation of the Fourier series approximations for each wave function, while the other manages the temperature distribution graphs. The flowchart for graph rendering is shown in Fig. 7.

Initially, the analytical sine and exponential decay terms representing heat transfer are evaluated for each Fourier mode across a discretized spatial and temporal domain. Each harmonic contribution is computed and stored in a structured 3D buffer indexed by term number, spatial position, and time step. This organization supports efficient summation of harmonic contributions and enables interactive modification of the number of terms, allowing users to observe Fourier convergence behavior in real time. Following computation, summation across the calculated terms is performed to reconstruct the approximated functions, with results stored in a grid structure where each cell corresponds to a unique pair of spatial and temporal coordinates. This grid-based approach contributes to the mesh generation of the graphs and real-time rendering in VR as per the selected wave function and number of terms.

The second script deals with the visualization and rendering of the computed data. It constructs a 3D surface mesh by mapping spatial position, temperature and temporal evolution to the x, y, and z axes, respectively. Mesh vertices, triangle indices, and per-vertex color values are generated with careful indexing to ensure a continuous and accurate surface representation. Dynamic scaling, orientation, axis construction, and labeling are incorporated to guarantee proper spatial placement of the 3D plot within the VR scene. In addition, this script enables interactive navigation and parameter adjustment through sliders, allowing users to intuitively explore temperature distribution graphs in a classroom-simulated VR environment. All computations related to Fourier harmonic calculation, summation, and mesh generation are handled by the CPU, while rendering operations such as mesh shading, lighting, and pixel-level coloring are offloaded to the GPU.

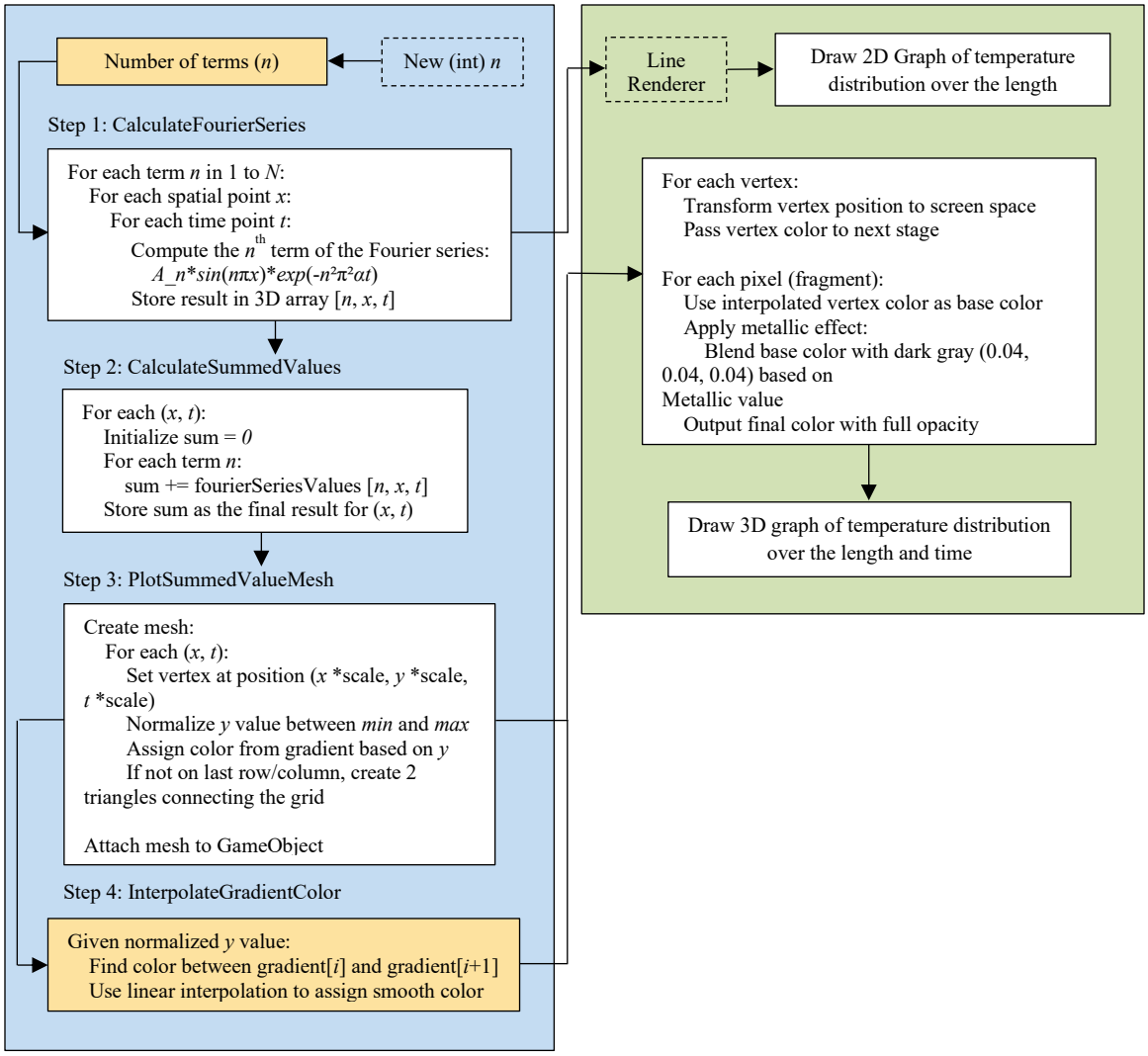


Fig. 7. Flow chart of graph rendering.

The temperature distribution surface is represented as a triangular mesh, which is the fundamental geometric structure used in real-time rendering (Angel Shreiner 2014). In this VR system, a 3D graph of the temperature distribution over length and time is discretized into a dense triangular mesh, as shown in Fig. 8. The zoomed-in view highlights the triangular tessellation of the temperature surface. The polygon count for the temperature distribution graph ranges from approximately 118k to 119k triangles, as reported directly by the Unity engine during runtime. This variation occurs due to dynamic mesh regeneration when parameters such as the number of Fourier terms, spatial resolution, or wave functions are modified interactively. The selected polygon range provides a balance between geometric accuracy and real-time performance. For the 2D graph generation, a line-rendering approach is employed. In this case, the curve is rendered

using a fixed set of 100 coordinate points, which are sufficient to accurately represent the 2D graph while keeping rendering costs minimal.

Besides generating the surface for a 3D graph, temperature variation along the bar length and over time is represented through a heat map with a color legend. To achieve this, a custom shader is applied to the surface mesh. A predefined color gradient is used to visually represent the magnitude of temperature across the distribution. Vertex amplitudes are normalized between the minimum and maximum temperature values and mapped to a predefined gradient sequence in the graph-plotting script. The heat map colors transition smoothly through intermediate colors. This per-vertex color interpolation ensures the smooth transition of intermediate colors as temperature varies.

The custom shader for heat map representation is developed in Unity. It utilizes per-vertex color data passed from the CPU-generated mesh, allowing each vertex to independently represent temperature intensity. The vertex program transforms each mesh vertex from object space to stereo-correct clip space while passing per-vertex color information to the fragment stage for accurate temperature visualization. It is equipped for stereo rendering using Unity's single-pass stereo mode, ensuring stereoscopic display by correctly transforming vertex positions for both eyes.

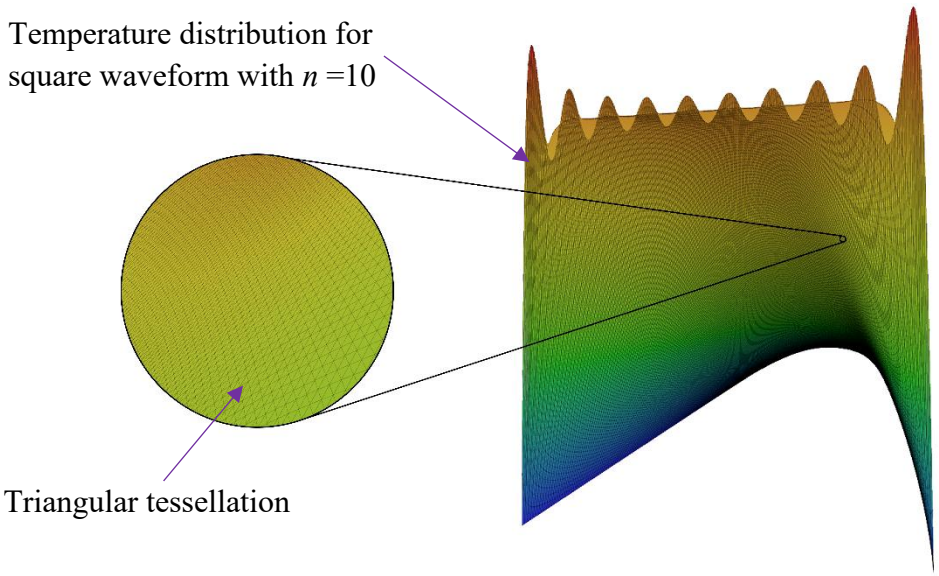


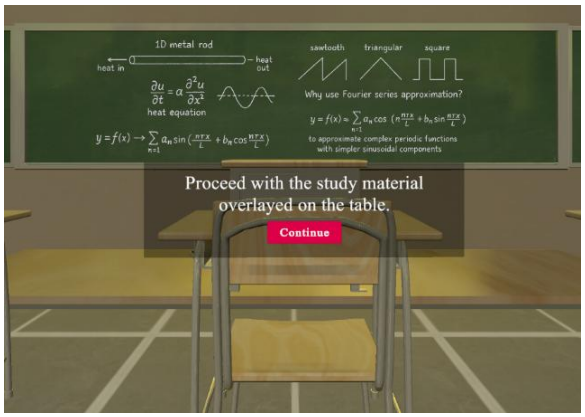
Fig. 8. Mesh structure of the temperature distribution surface.

4.3 VR-based user interface

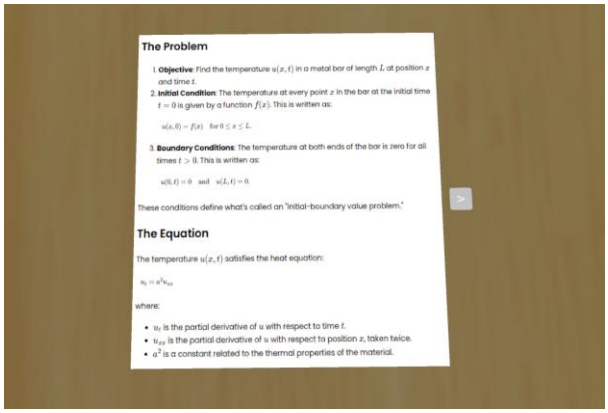
This system is designed by incorporating usability and design principles to ensure the intuitiveness, learnability, consistency and affordance. The sequence of interactions with the VR interface to learn the fundamentals of the heat equation and its solution is illustrated in Fig. 9.

Fig. 9(a) shows the stereoscopic virtual classroom viewed by the user with basic mathematical expressions presented on the board. The user can proceed to the next step by clicking the 'continue' button. This leads the user to look at his desk and study the mathematical expression of the general heat equation along with the initial and boundary conditions (Fig. 9(b)). Upon clicking the button with the 'next' symbol, Fig. 9(c) shows the user's first-person view from the HMD, indicating the buttons to proceed with three types of waves. Fig. 9(d) shows the third-person view of the learning environment. Next, Fig. 9(e) and (f) demonstrate the practical meaning of the chosen wave function. The user is instructed to proceed to visualize 2D and 3D graphs. The user can adjust the number of terms using an interactive slider with values ranging from 1 to 10, as shown in Fig. 9(g) and (i). Additionally, the graph scale can be doubled using the UI buttons below the slider (Fig. 9(g) and (i)) for better observation. The 2D and 3D graphs of temperature distribution for the corresponding number of terms are displayed to the user as shown in Fig. 9(h) and (j).

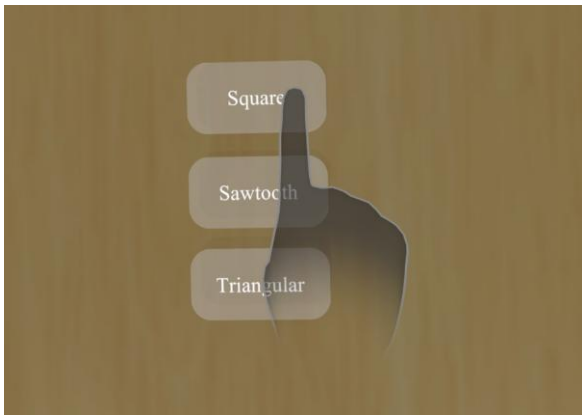
The system offers a smooth, seamless, and interactive user interface that allows users to visualize the temperature distribution graphs in real time by dynamically adjusting the number of terms and the type of wave functions.


1D metal rod
heat in
heat out
heat equation
sawtooth
triangular
square
Why use Fourier series approximation?
to approximate complex periodic functions with simpler sinusoidal components
Proceed with the study material overlayed on the table.
Continue

(a)


The Problem
1. Objective: Find the temperature $u(x,t)$ in a metal bar of length L at position x and time t.
2. Initial Condition: The temperature at every point x in the bar at the initial time $t = 0$ is given by a function $f(x)$. This is written as:
$u(x,0) = f(x)$ for $0 \le x \le L$.
3. Boundary Conditions: The temperature at both ends of the bar is zero for all times $t > 0$. This is written as:
$u(0,t) = 0$ and $u(L,t) = 0$.
These conditions define what's called an "initial-boundary value problem."
The Equation
The temperature $u(x,t)$ satisfies the heat equation:
$u_t = \alpha^2 u_{xx}$
where:
u_t is the partial derivative of u with respect to time t.
u_{xx} is the partial derivative of u with respect to position x, taken twice.
α^2 is a constant related to the thermal properties of the material.

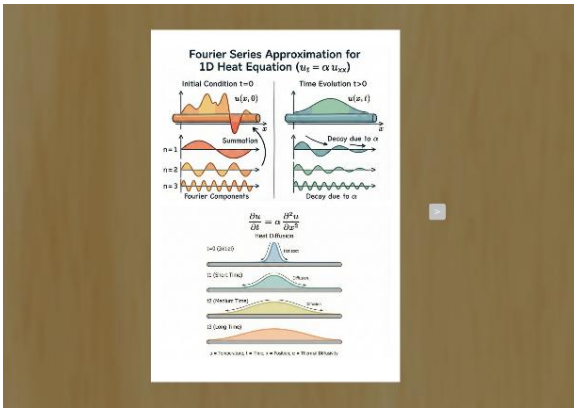
(b)


Square
Sawtooth
Triangular

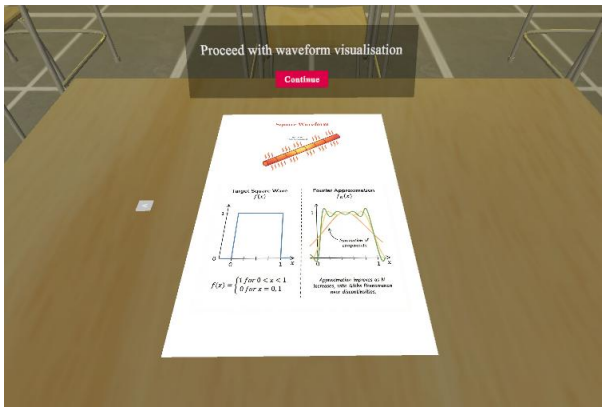
(c)



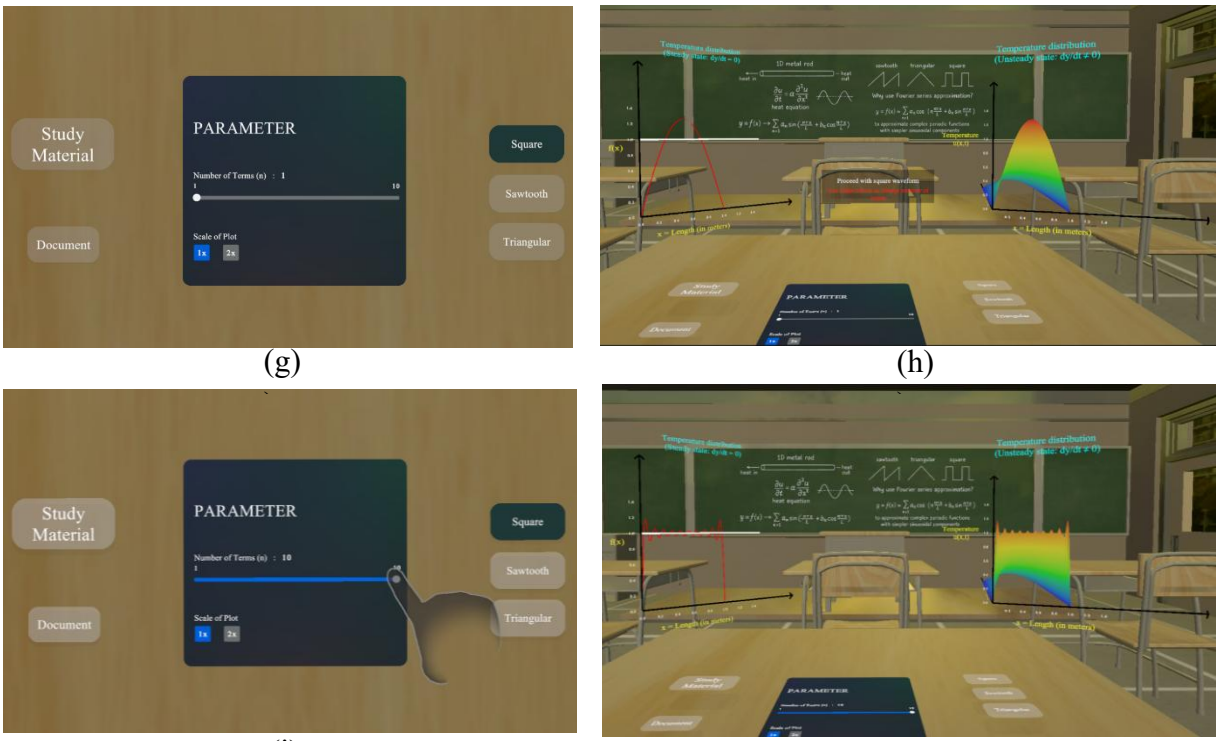
(d)


Fourier Series Approximation for 1D Heat Equation ($u_t = \alpha u_{xx}$)
Initial Condition t=0
Time Evolution t>0
Summation
Decay due to α
Fourier Components
Decay due to α
Heat Diffusion

(e)


Proceed with waveform visualisation
Continue

(f)



(g) (h)

(i) (j)

Fig. 9. User interface of VR-based tutorial system for fundamentals of heat equation.

5. User study

A user study was conducted to evaluate the learnability, usability, and performance of the VR system. The system is evaluated by comparing user performance results across two groups, namely VR group and control (CR) group. The VR group received the tutorial through the VR system and the CR group received it in a traditional classroom lecture with a class board explanation. The tutorial performance was evaluated using a written test and the system usability scale (SUS) for learnability and usability, respectively. The sample size of the participants was chosen to be thirty as suggested in prior studies for comparative tests (Faul et al. 2007; Nielsen Landauer 1993; Sauro Lewis 2016; Shankhwar Smith 2022). Participants were predominantly first-year engineering students, randomly selected to ensure they had no prior knowledge of the fundamentals of the heat equation, thereby eliminating potential bias in the results. Finally, 6 female and 24 male participants aged between 18 and 30 were recruited, with the majority (~83%) in the 18-25 age group.

Thirty participants were divided into two groups, with fifteen in each. The VR group finished the tutorial in 15 minutes, and the CR group finished it in 17 minutes. The CR group required an additional two minutes because participants were allowed to ask questions during the tutorial, whereas the VR system was self-explanatory. Immediately after the tutorial, a 5-minute written test was conducted for both groups to assess their knowledge retention from the tutorial. Participants in the VR group also filled out the SUS form for the system usability evaluation.

6. Results

6.1 Written test

The written test was administered after the tutorial to quantify the knowledge retained by participants in both groups and to evaluate the learnability of the system. The written test questions are designed based on the tutorial content, with reference to the prior books and relevant literature (Farlow 1993; Skinner 2016). The written test comprises 10 questions, with each question carrying 1 mark, as shown in Table 1. The test consists of two sections, theoretical and analytical, with multiple-choice questions.

The average scores obtained by the VR group and CR group are $M_1 = 5.6$ ($SD = 2.09$) and $M_2 = 3.67$ ($SD = 1.71$), respectively. Fig. 10 reveals that the range of the scores obtained by the VR group is 1–8, whereas the score range for the CR group is 0–6. Apart from this, the maximum number of participants in the CR group scored in the range of 3.1–4, while in the VR group scored in the range of 7.1–8. The scores of both groups are normally distributed, as confirmed by the Kolmogorov–Smirnov test. Parametric *t*-test results reveal that the score obtained by the VR group is significantly higher than that of the CR group ($p < 0.01$) with $\alpha = 0.05$.

Fig. 11 shows the comparison between the scores of two groups for the theoretical and analytical sections of the written test. The result deduced that the participants in VR performed significantly better than the CR group in the analytical section ($p < 001$). Nevertheless, no significant difference between the two groups was obtained in the theoretical section.

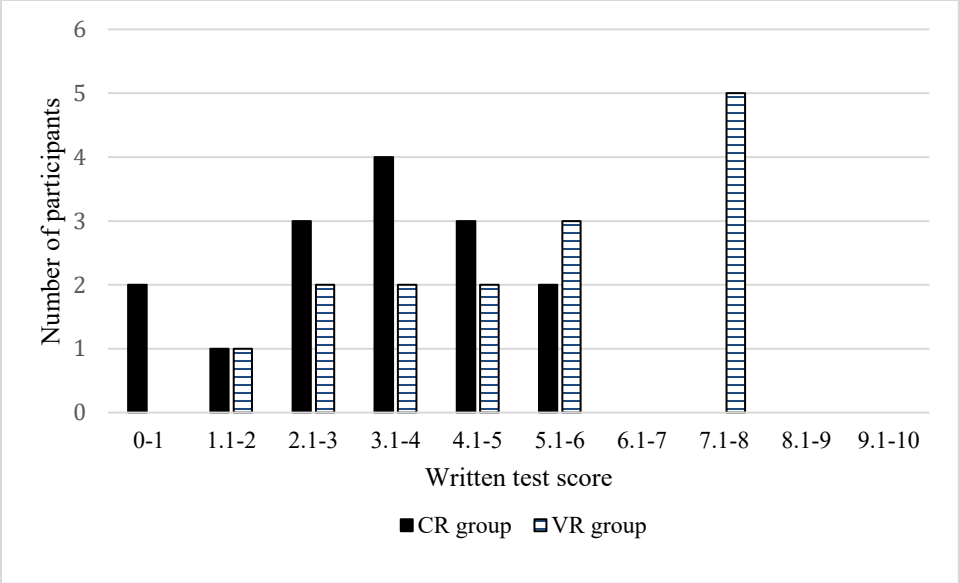


Fig. 10. Frequency distribution chart for the CR and VR groups.

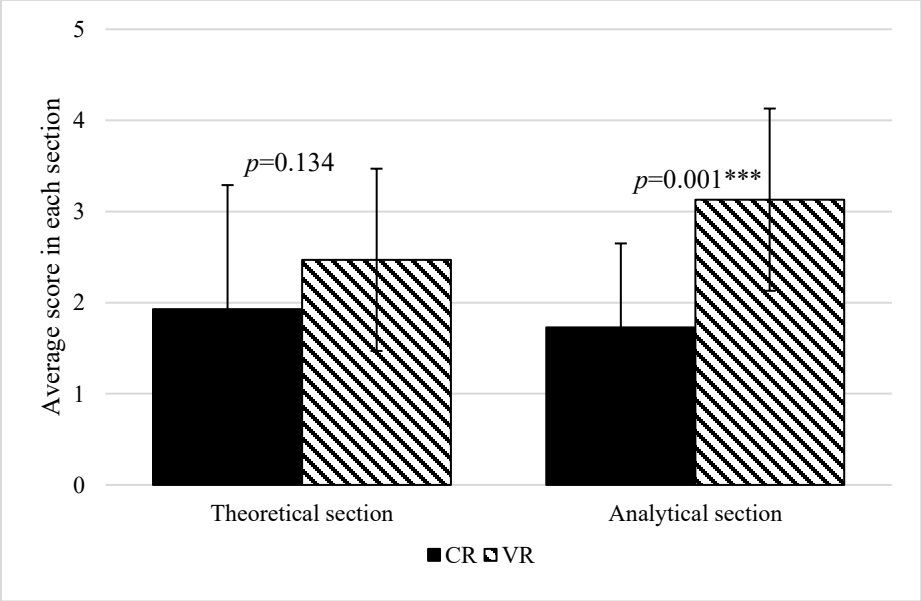


Fig. 11. Section-wise written test score results (*** ≡ $p \leq 0.001$, ** ≡ $p \leq 0.01$, * ≡ $p \leq 0.05$).

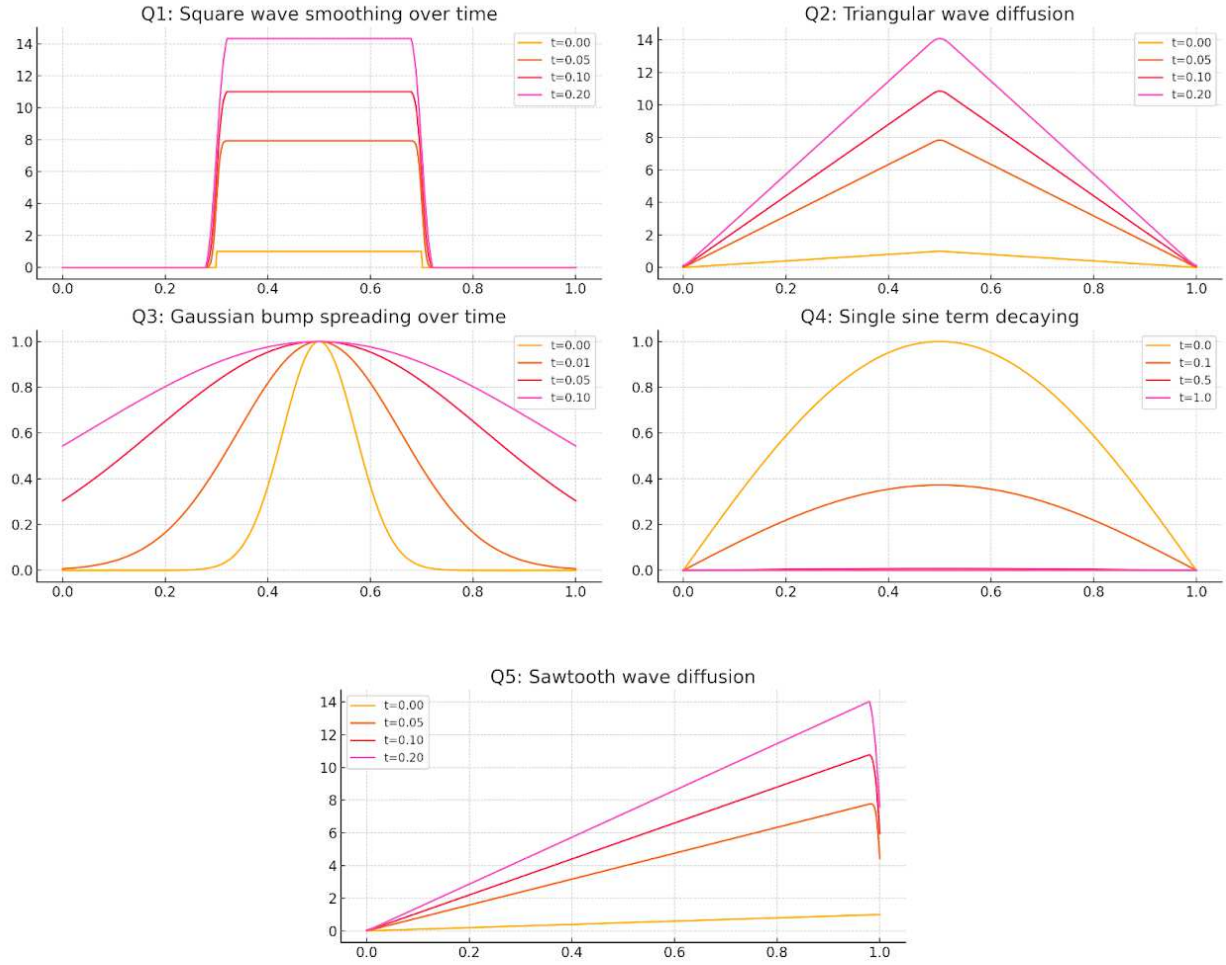
Table 1. Written test questions.

Section 1: Theoretical MCQs	
No.	**Questions**
1	According to the tutorial content, heat flow in the metal bar occurs because of: a. The bar's magnetic properties b. Differences in temperature c. External forces d. Inconsistent chemical compositions
2	Fourier's Law of heat conduction states that the heat flux is proportional to: a. Thermal diffusivity b. Temperature c. Temperature gradient d. Time
3	In solving the heat equation by separation of variables, the spatial solution involves sine functions mainly due to: a. The exponential nature of heat decay b. The periodic nature of the Fourier series c. Typical boundary conditions imposed on a finite bar d. Linear relationship between heat flux and temperature gradient
4	As $t \to \infty$, what happens to the solution $u(x,t)$? a. Approaches uniform temperature b. Increases indefinitely c. Becomes oscillatory d. Becomes discontinuous
5	What determines the Fourier coefficients in heat equation solutions? a. Boundary condition b. Initial temperature $u\ (x, 0)$ c. Diffusivity d. Length of the bar
Section 2: Analytical and reasoning MCQs	

6	You are given a graph of $u(x, t)$ at different time points (t = 0, 1, 2, 5). The initial shape is a square wave, and over time, the graph becomes increasingly smooth. What initial condition and behavior does this most likely represent? a. Smooth Gaussian wave; decays slowly b. Square wave; high-frequency components decay rapidly c. Triangular wave; exponential rise d. Sine wave; no change in shape
7	A triangular wave is given as $u(x,0)$. Which of the following best depicts the graph of $u(x, t)$ as t increases? a. Remains triangular b. Turns into a sine wave c. Becomes rounded and approaches a constant d. Oscillates with sharp peaks
8	You are shown four plots of $u(x, t)$ for various t. One plot shows a smooth, bell-shaped curve centered at $x = L/2$, remaining centered while its height decreases and width increases. Which initial condition is most likely? a. Square wave b. Gaussian temperature bump c. Sinusoidal function d. Triangular wave
9	You see a Fourier series where only the sine term is present: $u(x, t) = \sin(\pi x/L)e^{-a^2\left(\frac{\pi}{L}\right)^2 t}$. Which of the following is true? a. Multiple frequencies initially b. Initial temp $\propto \sin(\pi x/L)$ c. Heat does not decay d. Insulated boundaries
10	Given: $u(x, 0)$ = Sawtooth wave. At time $t = 0.5$, what change do you expect in the temperature graph? a. Sharp corners persist b. Edges will smooth due to the decay of high-frequency terms c. Oscillations will appear

	d. The wave will flatten the graph completely

Note: Visual graphs for Section 2 (Analytical & Graph-Based MCQs) are illustrated below, where the x-axis represents the position along the bar (typically 0 to 1), and the y-axis represents $u(x, t)$, the temperature at position x, for time t.



6.2 System usability scale

SUS is a global assessment tool of usability and learnability of a system (Lewis Sauro 2009). The SUS questionnaire consists of 10 statements, with 5-point Likert scale scoring of each statement ranging from 1 (strongly disagree) to 5 (strongly agree). Table 2 shows the SUS analysis results. The results in Table 2 reveal that in this study, the overall SUS mean score is 77.8, which

is higher than the average score of 70 (Derisma 2020), indicating acceptability, ease of use and users' satisfaction towards the VR-based tutorial system.

Table 2. Questionnaire results for SUS.

	SUS	Mean	SD
1	I think that I would like to use this system frequently	4.1	0.72
2	I found the system unnecessarily complex	1.5	0.88
3	I thought the system was easy to use	3.0	0
4	I think that I would need the support of a technical person to be able to use this system	2.5	1.31
5	I found the various functions in this system were well integrated	4.5	0.62
6	I thought there was too much inconsistency in this system	1.7	1.07
7	I would imagine that most people would learn to use this system very quickly	4.4	0.71
8	I found the system very cumbersome to use	1.7	0.87
9	I felt very confident using the system	4.4	0.61
10	I needed to learn a lot of things before I could get going with this system	2.0	1.26
	Total Score	77.83	

7. Discussion

Analysis of the written test results shows consistent improvement in participant performance, thereby validating its learnability. The overall score of the VR group is significantly higher than that of the CR group.

The section-wise comparison indicates that the VR group performs significantly better in the analytical section. It is because VR-based learning helps users visualize graphs from all angles and intuitively interact with parameters that dynamically modify graphs in real time. The analytical section includes questions that require knowledge of variation in the shape of graphs along the z-axis, which users effectively attained in the VR environment. Consequently, it leads to comprehensive learning and knowledge retention through an engaging and playful experience in a VR environment.

In contrast, no statistically significant difference is observed between the two groups in the theoretical section. The reason is that the VR group acquires theoretical concepts through 2D representations, including content displayed on a virtual class board and virtual handouts displayed at the users' desks, which is similar to the traditional classroom experience.

The system's usability is assessed using the SUS analysis. The SUS mean score is above the accepted average, confirming the system's learnability and usability for its intended purpose (Bangor et al. 2009). The SUS results indicate that the mean scores for the positive statements (odd-numbered) are above 4, except for statement 3. In contrast, most of the mean scores are below 2 for the negative statements (even-numbered). The mean score for statement 3 indicates a neutral user response, which may be attributed to the lack of prior experience with VR systems, leading to initial challenges in interaction.

Participants were asked open-ended questions during an unstructured interview to provide feedback on the VR system. The remarks provided by the participants are as follows: "It was fun to use this innovative learning tools with more engaging experience than traditional learning method, I feel the system is very intuitive and easy to use, a small description of each concept at a constant window should have been provided along with some video tutorials in the VR setup, other interactive features such as graph rotation and displacement could be provided, the VR system exceeded my expectations for aiding conceptual comprehension in an effective and intuitive manner".

8. Conclusion

The heat equation is typically taught using 2D board representations in traditional classrooms. This makes it difficult for students to visualize concepts such as 3D temperature distributions, limiting intuitive understanding and long-term retention. This study addresses this challenge by developing a tutorial system that facilitates the learning of the heat equation and its solution using Fourier series approximations for three types of waves: square, sawtooth, and triangular. Users can dynamically modify the wave function and Fourier terms to observe real-time changes in graphs. This is achieved by implementing a custom shader and 3D surface mesh rendering for 3D graph representation in VR. The performance of the VR system was evaluated by conducting a user study. The results indicated that the system's learnability and usability were satisfactory. The written test results revealed that the system can help students effectively retain knowledge of the

heat equation. Future work can focus on including elliptic and hyperbolic partial differential equations. In addition, a more interactive and self-explanatory system can be built by integrating large language models that can enable users to ask questions and receive real-time responses.

References

Alipour, S, Rah, A, Karki, B, Burris, J, Coward, L & Liao, T (2024) Enhancing Physics Education: Designing Customized Virtual Reality for Teaching Crystalline Structures. In: IEEE International Symposium on Mixed and Augmented Reality Adjunct (ISMAR-Adjunct), pp.549-552. Bellevue, WA, USA. https://doi.org/10.1109/ISMAR-Adjunct64951.2024.00158

Angel, E & Shreiner, D (2014) Interactive Computer Graphics: A Top-down Approach with WebGL. Pearson,

Bangor, A, Kortum, P & Miller, J (2009) Determining what individual SUS scores mean: Adding an adjective rating scale. Journal of Usability Studies 4:114-123.

Castillo, J F V, Santiago, L B & García, S M (2025) Optimization of Physics Learning Through Immersive Virtual Reality: A Study on the Efficacy of Serious Games. Applied Sciences, 15:3405. https://doi.org/10.3390/app15063405

Cheong, K H & Koh, J M (2018) Integrated virtual laboratory in engineering mathematics education: Fourier theory. IEEE Access, 6:58231-58243. https://doi.org/10.1109/ACCESS.2018.2873815

Cheong, K H, Lai, J W, Yap, J H, Cheong, G S W, Budiman, S V, Ortiz, O, Mishra, A & Yeo, D (2023) Utilizing Google cardboard virtual reality for visualization in multivariable calculus. IEEE Access, 11:75398-75406. https://doi.org/10.1109/ACCESS.2023.3281753

Derisma, D (2020) The usability analysis online learning site for supporting computer programming course using system usability scale (SUS) in a university. International Journal of Interactive Mobile Technologies, 14:182-195. https://doi.org/10.3991/ijim.v14i09.13123

Eynde, S V d, Schermerhorn, B P, Deprez, J, Goedhart, M, Thompson, J R & Cock, M D (2020) Dynamic conceptual blending analysis to model student reasoning processes while integrating mathematics and physics: A case study in the context of the heat equation.

Physical Review Physics Education Research, 16:010114. https://doi.org/10.1103/PhysRevPhysEducRes.16.010114

Farlow, S J (1993) Partial differential equations for scientists and engineers. Dover Publications, New York.

Faul, F, Erdfelder, E & Lang, A-G (2007) G* Power 3: A flexible statistical power analysis program for the social, behavioral, and biomedical sciences. Behavior Research Methods, 39:175-191. https://doi.org/10.3758/BF03193146

Frank, J A & Kapila, V (2017) Mixed-reality learning environments: Integrating mobile interfaces with laboratory test-beds. Computers & Education, 110:88-104. https://doi.org/10.1016/j.compedu.2017.02.009

Geng, G, Green, K, Telford, A, Zhu, Y J J o S E & Technology (2026) Engaging Young Minds: How Smart Augmented Reality Glasses Transform Learning Experiences in AR smart glasses Immersive Virtual Learning Environments (AR smart glasses IVLE). Journal of Science Education and Technology 1-20. https://doi.org/10.1007/s10956-026-10299-4

Ghazali, A K, Aziz, N A A, Aziz, K A & Kian, N T (2024) The usage of virtual reality in engineering education. Cogent Education, 11. https://doi.org/10.1080/2331186X.2024.2319441

Gorguis, A & Chan, W K B (2008) Heat equation and its comparative solutions. Computers & Mathematics with Applications, 55:2973-2980. https://doi.org/10.1016/j.camwa.2007.11.028

Guzmán, J D, Guzmán, D E & Rengifo, C F (2024) Use of Virtual Reality in the Teaching of Industrial Instrumentation. IEEE Revista Iberoamericana de Tecnologias del Aprendizaje, 19:212 - 219. https://doi.org/10.1109/RITA.2024.3471980

Han, Y (2022) Virtual reality in engineering education. In: International Conference on Educational Science and Social Culture (ESSC 2022), pp.02001. Kunming, China. https://doi.org/10.1051/shsconf/202315702001

Hou, H (2023) Enhancing indoor thermal comfort education: A virtual reality platform introducing Fanger's Model. In: Proceedings of the 2023 International Conference on Information Education and Artificial Intelligence, pp.948-952. Xiamen, China. https://doi.org/10.1145/3660043.3660212

Huang, K-T, Ball, C, Francis, J, Ratan, R, Boumis, J & Fordham, J (2019) Augmented versus virtual reality in education: An exploratory study examining science knowledge retention when using augmented reality/virtual reality mobile applications. Cyberpsychology, Behavior, and Social Networking, 22:105-110. https://doi.org/10.1089/cyber.2018.0150

Kumar, D S (2008) Heat & Mass Transfer. S. K. Kataria & Sons, New Delhi.

Lewis, J R & Sauro, J (2009) The factor structure of the system usability scale. In: International conference on human centered design, pp.94-103. San Diego. https://doi.org/10.1007/978-3-642-02806-9_12

Lindgren, R, Tscholl, M, Wang, S, Johnson, E & education (2016) Enhancing learning and engagement through embodied interaction within a mixed reality simulation. Computers & Education, 95:174-187. https://doi.org/10.1016/j.compedu.2016.01.001

Macariu, C, Iftene, A & Gîfu, D (2020) Learn chemistry with augmented reality. Procedia Computer Science, 176:2133-2142. https://doi.org/10.1016/j.procs.2020.09.250

Matovu, H, Won, M, Hernandez-Alvarado, R B, Ungu, D A K, Treagust, D F, Tsai, C-C, Mocerino, M, Tasker, R J J o S E & Technology (2024) The perceived complexity of learning tasks influences students' collaborative interactions in immersive virtual reality. Journal of Science Education and Technology 33:542-555. https://doi.org/10.1007/s10956-024-10103-1

Nielsen, J & Landauer, T K (1993) A mathematical model of the finding of usability problems. In: Proceedings of the INTERACT'93 and CHI'93 conference on Human factors in computing systems, pp.206-213. Amsterdam, Netherlands. https://doi.org/10.1145/169059.169166

Oje, A V, Hunsu, N J & May, D (2023) Virtual reality assisted engineering education: A multimedia learning perspective. Computers & Education: X Reality, 3:100033. https://doi.org/10.1016/j.cexr.2023.100033

Sauro, J & Lewis, J R (2016) Quantifying the user experience: Practical statistics for user research. Morgan Kaufmann, Cambridge.

Shankhwar, K, Chuang, T-J, Tsai, Y-Y & Smith, S (2022) A visuo-haptic extended reality–based training system for hands-on manual metal arc welding training. The International Journal of Advanced Manufacturing Technology, 121:249-265. https://doi.org/10.1007/s00170-022-09328-4

Shankhwar, K & Smith, S (2022) An interactive extended reality-based tutorial system for fundamental manual metal arc welding training. Virtual Reality, 26:1173-1192. https://doi.org/10.1007/s10055-022-00626-6

Simonetti, M, Perri, D, Amato, N & Gervasi, O (2020) Teaching math with the help of virtual reality. In: International Conference on Computational Science and Its Applications, pp.799-809. Cagliari, Italy. https://doi.org/10.1007/978-3-030-58820-5_57

Singh, G, Singh, G, Tuli, N & Mantri, A (2024) Hyperspace AR: an augmented reality application to enhance spatial skills and conceptual knowledge of students in trigonometry. Multimedia Tools and Applications, 83:60881-60902. https://doi.org/10.1007/s11042-023-17870-w

Skinner, D (2016) Mathematical Methods. https://www.damtp.cam.ac.uk/user/dbs26/1Bmethods.html. Accessed 10 February 2026

Streveler, R A, Litzinger, T A, Miller, R L & Steif, P S (2008) Learning conceptual knowledge in the engineering sciences: Overview and future research directions. Journal of Engineering Education, 97:279-294. https://doi.org/10.1002/j.2168-9830.2008.tb00979.x

Strzys, M P, Kapp, S, Thees, M, Klein, P, Lukowicz, P, Knierim, P, Schmidt, A & Kuhn, J (2018) Physics holo. lab learning experience: using smartglasses for augmented reality labwork to foster the concepts of heat conduction. European Journal of Physics, 39:035703. https://doi.org/10.1088/1361-6404/aaa8fb

Su, Y-S, Cheng, H-W & Lai, C-F (2022) Study of virtual reality immersive technology enhanced mathematics geometry learning. Frontiers in Psychology, 13:760418. https://doi.org/10.3389/fpsyg.2022.760418

Turkan, Y, Radkowski, R, Karabulut-Ilgu, A, Behzadan, A H & Chen, A (2017) Mobile augmented reality for teaching structural analysis. Advanced Engineering Informatics, 34:90-100. https://doi.org/10.1016/j.aei.2017.09.005